Diffusional Transport of Ions in Plasticized Anion-Exchange Membranes

ARTICLE *in* THE JOURNAL OF PHYSICAL CHEMISTRY B · MAY 2011

Impact Factor: 3.3 · DOI: 10.1021/jp1103615 · Source: PubMed

9 AUTHORS, INCLUDING:

Rakesh Kumar
Bhabha Atomic Research Centre
7 PUBLICATIONS **44** CITATIONS
SEE PROFILE

Ashok K Pandey
Bhabha Atomic Research Centre
106 PUBLICATIONS **1,234** CITATIONS
SEE PROFILE

Asimananda Goswami
Saha Institute of Nuclear Physics
265 PUBLICATIONS **1,811** CITATIONS
SEE PROFILE

THE JOURNAL OF PHYSICAL CHEMISTRY B

ARTICLE

pubs.acs.org/JPCB

Diffusional Transport of Ions in Plasticized Anion-Exchange Membranes

Rakesh Kumar,[†] Ashok K. Pandey,[*,‡] Manoj K. Sharma,[§] L. V. Panicker,[⊥] Suparna Sodaye,[‡] G. Suresh,[†] Shobha V. Ramagiri,[∥] Jayesh R. Bellare,[∥] and A. Goswami[‡]

[†]Research Reactor Services Division, [‡]Radiochemistry Division, [§]Fuel Chemistry Division, and [⊥]Solid State Physics Division, Bhabha Atomic Research Centre, Mumbai-400 085, India

[∥]Department of Chemical Engineering, IIT Bombay, Powai, Mumbai-400 076, India

Supporting Information

ABSTRACT: Diffusional transport properties of hydrophobic anion-exchange membranes were studied using the polymer inclusion membrane (PIM). This class of membranes is extensively used in the chemical sensor and membrane based separation processes. The samples of PIM were prepared by physical containment of the trioctylmethylammonium chloride (Aliquat-336) in the plasticized matrix of cellulose triacetate (CTA). The plasticizers 2-nitrophenyl octyl ether, dioctyl phthalate, and tris(2-ethylhexyl)phosphate having different dielectric constant and viscosity were used to vary local environment of the membrane matrix. The morphological structure of the PIM was obtained by atomic force microscopy and transmission electron microscopy (TEM). For TEM, platinum nanoparticles (Pt nps) were formed in the PIM sample. The formation of Pt nps involved in situ reduction of $PtCl_6^{2-}$ ions with BH_4^- ions in the membrane matrix. Since both the species are anions, Pt nps thus formed can provide information on spatial distribution of anion-exchanging molecules (Aliquat-336) in the membrane. The glass transitions in the membrane samples were measured to study the effects of plasticizer on physical structure of the membrane. The self-diffusion coefficients (D) of the I^- ions and water in these membranes were obtained by analyzing the experimentally measured exchange rate profiles of $^{131}I^-$ with $^{nat}I^-$ and tritiated water with H_2O, respectively, between the membrane and equilibrating solution using an analytical solution of Fick's second law. The values of $D(I^-)$ in membrane samples with a fixed proportion of CTA, plasticizer, and Aliquat-336 were found to vary significantly depending upon the nature of the plasticizer used. The comparison of values of D with properties of the plasticizers indicated that both dielectric constant and viscosity of the plasticizer affect the self-diffusion mobility of I^- ions in the membrane. The value of $D(I^-)$ in the PIM samples did not vary significantly with concentration of Aliquat-336 up to 0.5 mequiv g^{-1}, and thereafter $D(I^-)$ increased linearly with Aliquat-336 concentration in the membrane. The self-diffusion coefficients of water $D(H_2O)$ in PIM samples were found to be 1 order of magnitude higher than the value of $D(I^-)$ and varied slightly depending upon the plasticizer present in the membrane. It was observed in electrochemical impedance spectroscopic studies of the PIM samples that diffusion mobility of NO_3^- ions was 1.66 times higher than that of I^- ions, and diffusion mobility of SO_4^{2-} ions was half of that for I^- ions. The theoretical interpretation of experimental counterions exchange rate profiles in terms of the Nernst−Planck equation for interdiffusion also showed higher diffusion mobility of NO_3^- ions in the PIM than Cl^-, I^-, and ClO_4^- ions, which have comparable diffusion mobility.

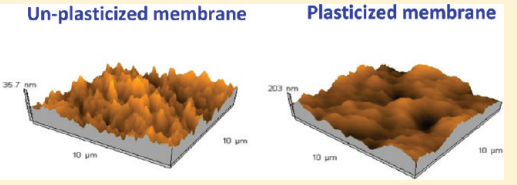

INTRODUCTION

Permeation selectivity, or perm-selectivity, of the membrane toward competing ions is an important factor for selective preconcentration of the target ions from multicomponent aqueous feed. Generally, the perm-selectivity is achieved by anchoring target ions specific functional groups (receptors) in the membrane. These membranes are termed as the functionalized membranes. The functionalized membranes are prepared by either physical containment or covalent attachment of the functional groups in a suitable organic or inorganic−organic hybrid matrix.[1,2] One of the simplest examples of a functionalized membrane system is the bulk liquid membrane (BLM) formed by the organic phase having ion-selective reagent between two aqueous phases.[3] The improved version of BLM is the supported liquid membranes (SLMs).[4] SLMs are formed by physical containment of the organic phase having an extractant in pores of the microporous host membrane. The capillary force stabilizes organic phase in the membrane matrix. This class of membranes has been found to be useful for small-scale applications in analytical chemistry.[5] However, a major drawback associated with SLMs is their poor stability for long-term applications.[6] The membrane can be made highly stable by linking functional groups covalently with the polymer chains. These membranes are synthesized by grafting the precursor chemical group

Received: February 2, 2010
Revised: March 29, 2011
Published: April 22, 2011

containing monomers on the poly(propylene) chains, and required functional groups are generated by subsequent chemical modification of the precursor chemical groups.[7] This class of membranes is termed as a fixed-site membrane. However, these membranes have not been successful for the facilitated transport of ions primarily because of slow transport rate across the membrane and also complicated synthetic chemistry involved in formation of the target specific receptors in the membrane.[8]

The intermediate of SLMs and fixed-site membranes is the polymer inclusion membrane (PIM), which is also used in the chemical sensors as solvent polymeric membrane.[9] These membranes are analogous to SLM but show better stability.[10] PIMs have been developed for a variety of applications in the separation science and chemical sensors.[9,11] In PIMs, the target specific reagent (extracting organic molecules) is contained in highly plasticized polymeric matrix. Poly(vinyl chloride) (PVC), cellulose triacetate (CTA), or their analogues are used as the matrix forming base polymer.[12,13] The base polymer forms a skeleton that provides mechanical strength to the PIMs. The chemical structure of the base polymer also plays an important role in transport of ions across the PIMs. For example, the polymer inclusion membranes containing bis-*tert*-butylcyclohexano-18-crown-6 as a metal cation carrier showed that flux of K^+ diminished with increasing size of the cellulose side chains.[13] However, the length of the alkyl side chain of cellulose has been found to influence stability of the PIM in acidic conditions.[13] The physical structure of the PIMs is a key issue in understanding the transport mechanism of ions across these membranes. Ye et al. have suggested three-dimensional grid structures for plasticized PVC membrane based on small-angle neutron scattering studies.[14] The AFM surface roughness profiles of the PIM, made up of plasticized CTA, seem to suggest a regular pattern of plasticized blobs of CTA nodes in the membrane.[15] X-ray diffraction spectra of the PIMs consisting of CTA, NPOE, and varying concentration of Lasalocid A were studied by C. Fontas et al.[16] It was found in this study that the XRD pattern of the crystalline part of CTA was not affected significantly on addition of the plasticizer 2-nitrophenyl octyl ether (NPOE). However, the amorphous part of the CTA diffraction pattern was altered. Transmission infrared mapping microspectroscopy of the PIM samples containing CTA, plasticizer NPOE or tris(2-ethylhexyl)-phosphate (TEHP), and carrier bis(2,4,4-trimethylpentyl)phosphinic acid (CYANEX 272) revealed that distribution of the carrier in the PIM was highly dependent on the hydrogen bonding and dipolar interactions of the carrier with plasticizer and matrix forming polymer CTA.[17]

Though selectivity of the PIMs (partition coefficient of the ions at aqueous−membrane interface) is governed by the chemical property of the carrier, the properties of the plasticizer like viscosity and dielectric constant strongly influence transport of the ions across the membrane.[9a,10a,18] The mechanism of solutes (ions/molecules) diffusion across the PIMs may occur through fixed-site jumping,[19,20] carrier-diffusion,[21] or mobile-site jumping depending upon the composition of the membrane.[22] In previous work from our laboratory, it was observed that the competition of the anions with the I^- ions for available exchange sites of the liquid anion-exchanger trioctylmethylammonium chloride in NPOE plasticized CTA matrix (PIM) was dependent upon the hydration energy of the anions and followed the pattern of the Hofmeister series.[18b,d] Malewitz et al. observed during competitive uptake of the anions in the Neosepta^R AMX and Selemion^R AMV anion-exchange membranes that the selectivity pattern of anions was NO_3^- > Br^- > Cl^-.[23] However, the selectivity in anions transport through polymer inclusion membranes facilitated by transition metal containing carriers was found to be dependent not only on their electrostatic interactions but also on the affinity of the carrier toward specific anion.[24]

In the present work, the diffusional transport properties of the PIMs with different compositions have been studied. The samples of PIM have been prepared by physical containment of a liquid anion-exchanger trioctylmethylammonium chloride (Aliquat-336) in the plasticized matrix of CTA. Three different plasticizers used in the PIMs are NPOE, dioctyl phthalate (DOP), and TEHP having different dielectric constant and viscosity. Since carrier and plasticizer are the important constituents of the PIM, the amounts of both have been varied in the samples to study the diffusion property. The PIM samples have been subjected to microscopic (AFM and TEM) and radiotracer studies to understand the effects of the plasticizer on physical structure and ion-exchange capacity of the membrane. Pt nanoparticles have been synthesized in the PIM sample for transmission electron microscopy (TEM). The Pt nps formed by using anionic species ($PtCl_6^{2-}$ and BH_4^-) are expected to provide information on distribution of anion-exchanges molecules (Aliquat-336) in the membrane. The glass transitions of the membrane samples have been studied to understand the effect of carrier (Aliquat-336) and plasticizer on the crystalline phase of cellulose triacetate used as the matrix forming polymer. The self-diffusion of ions in a homogeneous medium is due to continuous random motion of the ions that gives rise to a definite probability of arrival of a given ion at some point within a given time. Since there is no external gradient involved in the measurement of self-diffusion coefficients, intrinsic diffusional-transport properties of the membrane can be understood from the study of self-diffusion coefficients of the water and counterions. The most effective method for a experimental determination of self-diffusion coefficient is the isotopic-exchange method using radioactivity tagged species.[25] In present work, the self-diffusion coefficients of I^- anions (tagged with $^{131}I^-$) and water (tagged with ^3H) have been measured. The choice of I^- ions for the diffusion studies has been based on the fact that its pure radiotracer ^{131}I (free from nonradioactive iodine isotopes) is easily available, which has convenient γ-energy (364 keV) and half-life. The kinetics of I^- ion exchanges with Cl^-, NO_3^-, and ClO_4^- anions between the membrane sample and equilibrating solution have also been measured to study the diffusion rates of these ions with respect to the I^- ion. Electrochemical impedance spectroscopy (EIS) has been carried out to study electrical and diffusional properties of the PIM samples having different counterions. The selection of Cl^-, NO_3^-, ClO_4^-, and SO_4^{2-} ions for the diffusion studies has been based on the fact that these ions have systematic variation of degree of hydration and thus represent Hofmeister series from highly hydrated to less hydrated ions.[18b] The results obtained in the present work have been used to interpret the diffusional-transport process in the PIM.

EXPERIMENTAL SECTION

Material and Reagents. Analytical grade reagents and deionized water (18 MΩ/cm) purified by model Quantum^{TM} from Millipore (Mumbai, India) were used throughout the work. Cellulose triacetate (molecular weight 72 000−74 000, acetyl value = 43.2%), Aliquat-336, and 2-nitrophenyl octyl ether (NPOE) were obtained from Sigma-Aldrich (Steinheim, Germany).

Tris(2-ethylhexyl)phosphate (TEHP) (Koch-Light Laboratories, Coinbrook Bucks, England) and dioctyl phthalate (DOP) (BDH, Poole, England)) were used as obtained. These chemicals had high purity (>98%). The radiotracer $^{131}I^-$ used in the present work was obtained from the Board of Radiation and Isotope Technology, Mumbai, India. The aqueous solution containing $^{131}I^-$ ions was purified from I_2 by equilibration with chloroform. The stock solution was prepared by spiking 0.1 mol L^{-1} KI solution with a known radioactivity of purified $^{131}I^-$ radiotracer. The γ-ray activity of $^{131}I^-$ radiotracer (364 KeV) was monitored by using a well-type NaI(Tl) γ-ray detector connected to a multichannel analyzer. All the samples and standard containing radioactivity were counted in an identical geometry. β-radioactivity of the tritiated water (HTO) was measured by adding 50 μL of sample drawn from equilibrating solution to a vial containing 5 mL of scintillation cocktail-w (2,5-diphenyloxazole = 10 g, 1,4-di-2-(5-phenyloxazolyl)benzene = 0.25 g, naphthalene = 100 g in 1000 mL of 1,4-dioxane solvent), and counting β radioactivity in a vial with Packard Liquid Scintillation Analyzer (model TRI-CARB 2100 TR). The thicknesses of membrane samples were measured using a digital micrometer (Mitutoy, Japan) with an accuracy of $\pm$0.001 mm. The instrument used for carrying out the ac-impedance measurements was the AUTOLAB Frequency Response Analyzer 2 (Eco Chemie B. V., Utrecht, The Netherlands).

Preparation of Membrane. The details of preparation and characterization of the PIMs were described in our earlier publication.[18b] Briefly, a solution of cellulose triacetate (CTA) was prepared by dissolving CTA (0.2 or 0.4 g) in 5 mL of dichloromethane. A separate solution in dichloromethane (5 mL) containing known amounts of a plasticizer (0.2−0.6 g) and Aliquat-336 (0.05−0.25 g) was prepared. A casting solution was prepared by mixing the two solutions and homogenized by ultrasonication for 2 min. This casting solution was poured on a leveled 9 cm diameter flat bottom casting plate. Dichloromethane was allowed to evaporate slowly over a period of 2 days. After the evaporation of dichloromethane, the transparent membrane samples were peeled off from casting plates and annealed at 50 °C for 3 h to remove residual solvent. The membrane was cut into pieces of required dimensions for the experiments. The membrane samples were stored in 0.1 mol L^{-1} NaCl solution to keep them in Cl^- ionic forms.

Microscopy Characterization. For atomic force microscopy (AFM) studies of the membrane samples, tapping mode AFM measurements were performed at ambient temperature conditions using a Nanosurf easyScan 2 AFM (Nanosurf, Switzerland) with 10 μm scanner head. The cantilevers used were NCLR-10 (Nano World) with a resonance frequency of 190 kHz and force constant of 48 N/m. AFM data were analyzed using Nanosurf Report 4.1 software. The root-mean-square roughness (S_q) values of 100 μm^2 surface area of membrane samples were obtained by the following equation:

$$S_q = \sqrt{\frac{1}{MN}\sum_{k=0}^{M-1}\sum_{l=0}^{N-1}(Z(X_K Y_l))^2} \qquad (1)$$

The image was divided into a number of lines, and each line was further divided into a number of points. N is the number of measured data lines, and M is the number of measured data points per line in an image. In this case the number of measured data lines was equal to the number of measured data points per line, i.e., $N = M$. The data is acquired and stored at each point during the scan/measurement. $Z(X_k, Y^l)$ is the Z-position of the tip (local sample height) at the point with coordinates (k, l) in the image.

For TEM studies, the Pt nanoparticles were formed in the membrane samples. The details of metal nanoparticles formation in the PIMs are described elsewhere.[26] The membrane samples (2 × 2 cm) were equilibrated with 15 mL of 0.05 mol L^{-1} H_2PtCl_6 solution overnight. These $PtCl_6^{2-}$-loaded membrane samples were reduced by immersing them in 25 mL of well-stirred 0.1 mol L^{-1} $NaBH_4$ solution for 30 min at 25 °C. After reduction, the membrane samples were thoroughly washed with water and then conditioned with 0.1 mol L^{-1} NaCl. The cycle of loading of $PtCl_6^{2-}$ ions followed by reduction with BH_4^- ions was repeated five times to increase density of the nanoparticles. These membrane samples were sectioned across the thickness under cryogenic conditions in Leica ultramicrotome to 70 nm thickness. The sections were picked on 200 mesh Cu grids. The grids were examined in an FEI Technai G2 electron microscope at IIT Bombay (Central Facility at SAIF), Mumbai at 120 KeV without any staining or post-treatment. The X-ray diffraction (XRD) patterns of the Pt nps embedded membrane samples were recorded using a Philips X-ray diffractometer (model PW 710) with monochromatic Cu−K_α ($K_{\alpha1}$ = 1.5406 A° and $K_{\alpha2}$ = 1.5444 A°) radiations from an X-ray generator operated at 30 kV 20 mA. The instrumental line broadening was corrected using Si standard.

Differential Scanning Calorimetry (DSC). DSC was used to study the glass transitions in the membrane samples. DSC profiles were recorded at heating rate of 10 °C min^{-1} under inert atmosphere using a Mettler Toledo DSC 822 with an empty aluminum pan as the reference. Temperature and enthalpy calibration of the instrument were done using cyclohexane and indium. The transition temperature reported is the peak temperature. The transition enthalpy of the endothermic curve was calculated by using the software supplied by Mettler Toledo. About 7−8.5 mg membrane samples were used to record the scans.

Anion-Exchange Capacity. The total exchangeable sites (IES, in moles) available in the membrane samples (2 × 2 cm pieces) were measured by equilibrating them for 24 h with 15 mL of 0.05 mol L^{-1} KI stock solution containing known activity of ^{131}I radiotracer. The concentration of KI in the equilibrating solution was varied up to 0.1 mol L^{-1}. It was observed that the ion-exchange capacities of the membrane samples remained constant above 0.01 mol L^{-1} concentration of KI. The saturation equilibration time of membrane sample in well-stirred KI solution was found to be 45 min. However, 24 h equilibration of the membrane sample in 0.05 mol L^{-1} KI stock solution was carried to measure the ion-exchange capacity. After equilibration, the membrane samples were thoroughly washed with deionized water to remove equilibrating solution clinging to the surface of the samples. Filter paper standards were prepared by taking pieces of filter paper of the same dimensions (2 × 2 cm) as the membrane samples and spreading a known volume (50, 100, and 200 μL) of the radiolabeled 0.05 mol L^{-1} KI stock solution. KI stock solution used for preparing standard samples contained the same $^{131}I^-$ (radioactive) to $^{127}I^-$ (natural) ratio as in the solution used for equilibrating the membrane samples. Each standard was prepared in duplicate. The soaked filter papers were dried at room temperature and counted in a well type NaI(Tl) detector in a similar counting geometry as that used for the membrane samples. The amount of I^- ions in the membrane sample was obtained by comparing the γ-activity of $^{131}I^-$ in the membrane

Table 1. Comparison of Experimental and Calculated Ion-Exchange Capacities of the Membrane Samples with Varying Proportions of Different Plasticizers[a]

		composition (wt %)							
id.	plasticizer	CTA	Aliquat-336	plasticizer	density (g cm^{-3})	thickness (μm)	exp. I.E.C (mequiv g^{-1})	cal. IEC (mequiv g^{-1})	exp. I.E.C./cal. I.E.C.
C-1	none	100	–	–	1.18	32 ± 2	not detected	0	–
C-2	none	78.66	21.34	0	1.14	36 ± 2	0.44 ± 0.02	0.53	0.84
C-2	none[b]	79.85	20.15	0	–	70 ± 1	0.43	0.50	0.85
N-1	NPOE	55.99	16.24	27.78	1.06	55 ± 2	0.34 ± 0.03	0.40	0.84
N-2	NPOE	42.22	12.21	45.57	1.08	69 ± 1	0.28 ± 0.01	0.30	0.92
N-3	NPOE	36.11	9.84	54.05	1.17	76 ± 1	0.22 ± 0.02	0.24	0.90
T-1	TEHP	55.66	16.50	27.84	1.01	56 ± 2	0.37 ± 0.03	0.41	0.91
T-2	TEHP	44.29	11.50	44.21	0.99	72 ± 1	0.25 ± 0.01	0.28	0.88
T-3	TEHP	36.01	9.68	54.31	1.05	83 ± 1	0.21 ± 0.02	0.24	0.89
D-1	DOP	55.53	15.37	29.10	1.06	53 ± 2	0.30 ± 0.06	0.38	0.77
D-2	DOP	43.90	12.31	43.79	1.08	68 ± 1	0.26 ± 0.01	0.30	0.85
D-3	DOP	35.16	9.59	55.25	1.12	81 ± 1	0.21 ± 0.01	0.24	0.89

[a] The calculated ion-exchange capacities were obtained from the weight fraction of Aliquat-336 in casting solutions. The amounts of CTA and Aliquat-336 were kept as 0.2 and 0.05 g, respectively. [b] Thickness of the membrane sample was increased by doubling the contents of CTA and Aliquat-336 in casting solution.

samples with the filter paper standards as given below

$$\text{ion exchange sites} = \frac{A_{(\text{mem})}}{A_{(\text{std})}} \times M_{(\text{std})} \qquad (2)$$

where $A_{(\text{mem})}$ and $A_{(\text{std})}$ are $^{131}I^-$ γ-radioactivity (counts min^{-1}) in the membrane sample and standard, respectively. $M_{(\text{std})}$ is moles of I^- ions in the standard.

Measurements of Self-Diffusion Coefficients. The measurements of self-diffusion coefficients of I^- ions and water in the PIMs with different compositions were carried out using 2.5 × 2.5 cm pieces of samples. A membrane sample in the I^- ionic form was loaded with $^{131}I^-$ radiotracer ions as described elsewhere.[18c] The isotopic-exchange profiles were obtained by equilibrating the radiotracer-loaded membrane sample with 25 mL aqueous solution of 0.1 mol L^{-1} KI with constant stirring (≈400 rpm). The amount of radiotracer ions diffusing out of the membrane sample was monitored by taking out 50 μL samples of equilibrating salt solution at regular time intervals and counting their γ-activity. In some experiments, the radioactivity of $^{131}I^-$ diffusing in/out of the membrane was monitored by taking out the membrane sample for γ-activity measurements at different time intervals and placing it again in equilibrating solution. For the measurements of tritiated water (HTO) exchange rates, the PIM samples with I^- counterions were equilibrated with water containing known radioactivity of HTO overnight. The HTO-loaded PIM sample was immersed in a 25 mL of well-stirred deionized water (without HTO radiotracer) at 25 °C. The amount of radiotracer HTO diffusing out of the membrane sample was monitored by taking out 50 μL samples from the equilibrating deionized water at regular time intervals and measuring β-radioactivity of HTO by scintillation counting.

The exchange rate profiles of radioactivity tagged I^- ions/HTO diffusing out of the membrane samples in the well-stirred solution as a function of equilibrium time were analyzed by using an analytical solution of Fick's second law given below[25]

$$N(t_k) = N^*[1 - (8/\pi^2)\{\exp(-D\pi^2 t_k/L^2) + (1/9)\exp(-9D\pi^2 t_k/L^2) + ...\}] \qquad (3)$$

where $N(t_k)$ and N^* are the radioactivity of radiotracer ($^{131}I/^3H$) in the membrane sample or equilibrating solution at fixed time $t = t_k$ and infinite time t_∞, respectively, D is the self-diffusion coefficient of species in the membrane, and L is the thickness of the membrane. The initial and boundary conditions are described in our earlier publication.[25,29] The above equation is valid when there is no concentration gradient of the exchanging species (I^- ions/HTO) in the equilibrating solution. This means that there is negligible contribution of the aqueous diffusion in the exchange rates of I^- ions between the membrane sample and equilibrating solution. It has been reported elsewhere that the contribution from aqueous diffusion on the exchange rate profiles of stirred membrane sample (400 rpm) was negligible under the experimental conditions used in the present work.[25,29] The value of D was obtained by a nonlinear least-squares fit of the experimental exchange rate profile with the above equation keeping both N^* and D as the free parameters. $N(t_k)$ was measured as a function of equilibration time t_k by measuring radioactivity of the radiotracer-tagged species in membrane sample or equilibrating solution. The fractional attainment of exchange equilibrium $F(t)$ was obtained from the ratio of $N(t_k)$ to N^* as a function of the equilibration time t_k.

Electrochemical Impedance Spectroscopy. A small sine wave ac potential was applied to an electrochemical cell arrangement shown in the Supporting Information over a frequency range from 1 MHz to 10 Hz. The area of the membrane under study in the measuring cell exposed to mercury was 1.227 cm^2. Thus obtained impedance spectra were analyzed with help of the Frequency Response Analyzer software (Eco Chemie B.V., Utrecht, Netherlands). The equivalent circuit of the experiment is given in the Supporting Information. The runs were analyzed assuming that the membrane behaved as a parallel RC circuit in the frequency range used.[27] Bulk resistance of the membrane samples, loaded with different anions, was measured using same EIS experimental setup described above. For this experiment, the membrane samples were equilibrated with 0.1 mol L^{-1} salt solutions con taining Cl^-, NO_3^-, I^-, and SO_4^{2-} ions for 24 h. The self-diffusion coefficient of the anion in PIM sample was

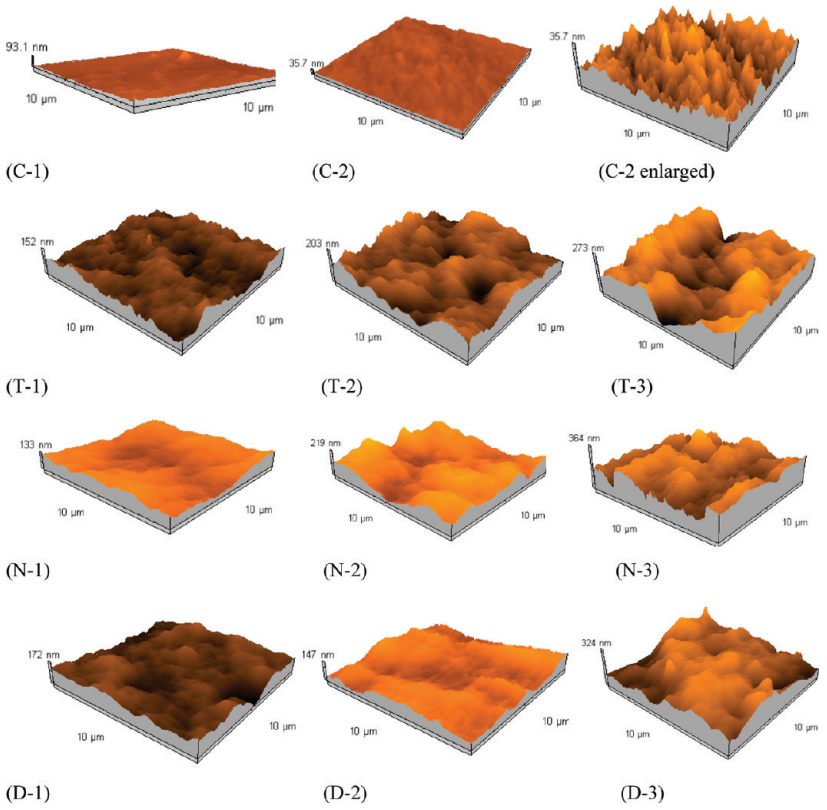

Figure 1. AFM images of the PIM samples with and without plasticizers. The compositions of samples are given in Table 1. The scales of *Z*-axis for all the images were kept the same except for the enlarged C-2 AFM image. C, T, N, and D series images are of the PIM samples without plasticizer and with TEHP, NPOE, and DOP plasticizers, respectively.

determined using the relation[28]

$$D = (kT/\bar{e}FAC)*(d/Rz^2) \quad (4)$$

where k is the Boltzmann constant, T is the absolute temperature in K, $\bar{e}$ is the charge of the electron, F is Faraday's constant, A is the area of the membrane, C is the concentration of anions in the membrane (=ion-exchange sites in the membrane sample), d is the thickness of the membrane, R is the bulk resistance of the membrane, and z is the charge on the anion. In present work, the values of D of anions were normalized with D values of I^- ion in the same membrane obtained by the radiotracer method.

Counterions Exchange Rates. The membrane samples having fixed dimensions were converted to required ionic forms by equilibrating these with aqueous sodium/potassium salt solutions containing 0.1 mol L^{-1} concentration of relevant anions. The quantitative displacements of anions in the membrane samples were monitored by using $^{131}I^-$ radiotracer. The counterions (X^- = NO_3^-, Cl^-, and ClO_4^-) exchanges with I^- ions between the membrane sample and well-stirred aqueous salt solution (0.1 mol L^{-1}) were measured using $^{131}I^-$ radiotracer-tagged I^- ions. Both forward exchange rate involving $(I^-)_m \rightleftarrows (X^-)_{aq}$ system and reverse exchange rate involving $(X^-)_m \rightleftarrows (I^-)_{aq}$ system were experimentally measured by monitoring the radioactivity of $^{131}I^-$ sorbed or desorbed in the membrane sample as a function of equilibration time in well-stirred appropriate salt solution.

RESULTS AND DISCUSSION

The compositions of PIMs studied in present work are given in Table 1. The densities and anion-exchange capacities of these membrane samples were measured. Density varied depending upon composition of the membrane sample. In general, the density of membrane sample decreased on addition of Aliquat-336 and plasticizer in its matrix. It is seen from the data given in Table 1 that the ion-exchange capacities varied systematically as a function of weight fraction of Aliquat-336 in the membrane sample. To understand the effect of plasticization on accessibility of the anion-exchanger molecules, ion-exchange capacities were calculated from the weight fraction of Aliquat-336 used in casting the membrane samples. The comparison of experimental and expected ion-exchange capacities given in Table 1 seems to indicate that 85% anion-exchange sites were exchangeable even in the absence of plasticizer. The addition of plasticizer slightly improved the ion-exchange capacity of the PIM to ≈90% of the expected ion-exchange capacity.

The AFM images of the membrane samples without plasticizer and with varying amounts of the different plasticizers are shown in Figure 1. The AFM images showed that the surface morphology changed significantly on addition of the plasticizer. The surfaces of membrane samples having only CTA (C-1) and CTA + Aliquat-336 (C-2) are almost flat. The enlarged AFM image of sample C-2 revealed surface roughness that appears like an egg basket. The small features seen in the AFM image of sample C-2 were swollen on addition of the plasticizer, which increased the surface roughness. The comparison of AFM images

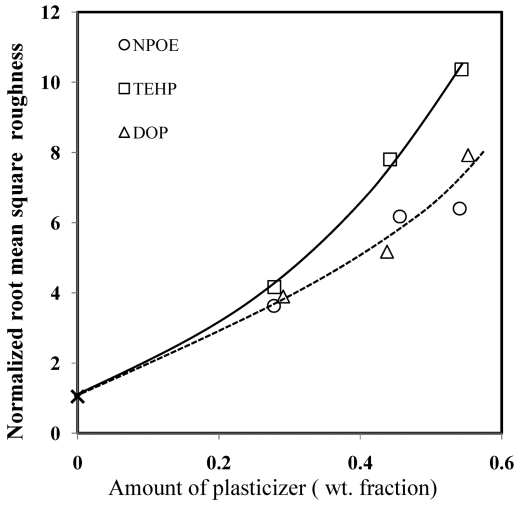

Figure 2. Variation of root-mean-square roughness (S_q) of the membrane samples, normalized with S_q of the sample made up of only CTA, as a function of weight fraction of the plasticizer. The membrane samples contained fixed proportion of CTA and Aliquat-336 as given in the Table 1.

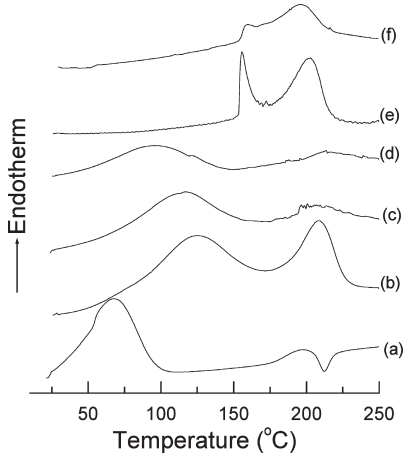

Figure 3. DSC heating thermograms of membrane samples containing (a) CTA only (C-1), (b) CTA+Aliquat-336 (C-2), (c) CTA+Aliquat-336+TEHP (T-1), (d) CTA+Aliquat-336+TEHP (T-3), (e) CTA+Aliquat-336+NPOE (N-3), and (f) CTA+Aliquat-336+DOP (D-3).

given in Figure 1 suggested that surface roughness of the membrane sample increased with amount of the plasticizer. In order to correlate the extent of surface roughness with the amount of plasticizer, the root-mean-square roughness (S_q) of the fixed area of the membrane samples having different plasticizers was plotted in Figure 2 as a function of the weight fraction of plasticizer. The values of S_q of different membrane samples in Figure 2 were normalized with the value of S_q of membrane sample containing only CTA (C-1). It is seen from the data that the value of S_q was marginally increased on addition of Aliquat-336 in the membrane. As can be seen from Figure 2, the value of S_q increased with amount of all three plasticizers studied in the present work. However, the increase in the value of S_q was higher in the membrane sample having TEHP than the other membrane samples having the same weight fraction of either DOP or

Table 2. Data Obtained from Differential Scanning Calorimetry of the Membrane Samples[a]

sample id.	T_{g1} (°C)	ΔH_{g1} (J g^{-1})	T_{g2} (°C)	ΔH_{g2} (J g^{-1})
C-1	68.1	55.2	196.6	4.3
C-2	122.5	43.3	208.7	26.6
T-1	116.5	40.7	210	8.9
T-3	95.4	26.0	212	6.0
N-3	overlapping peaks		155.6 and 202.8	53.6
D-3	overlapping peaks		158.3 and 195.9	24.1

[a] T_{g1} and T_{g2} are glass transition temperatures, and ΔH_{g1} and ΔH_{g2} are corresponding glass transition enthalpies.

NOPE. This suggested that plasticization of CTA is better with TEHP than with the other two plasticizers.

The rubber-to-glass transition temperature (T_g) of the polymeric film is dependent on structural, compositional, and conformational factors as well as on the degree of cross-linking, average molecular weight, presence of additives, stabilizers, and plasticizers in the polymeric matrix. Miguel et al. measured the T_g of the PIM made up of CTA, LIX^R 84-I (carrier), and tris (2-*n*-butoxyethyl)phosphate (plasticizer), which was found to be 175 °C.[9d] However, it was not clear how T_g had varied with respect to pure CTA and with addition of different components. Therefore, a systematic study was carried out to study change in T_g on addition of different components. The DSC thermograms were obtained at a heating rate of 10 °C min^{-1} in the temperature range 20−250 °C. The glass transition data obtained by analyses of DSC heating thermograms of PIM samples made up of CTA, CTA+Aliquat-336, and CTA+Aliquat-336+plasticizer (TEHP/NPOE/DOP) are given in Figure 3 and Table 2, respectively. It was observed that PIM containing only CTA had two T_g values corresponding to two different kinds of crystalline phases. It has been reported elsewhere that CTA has multiple glass transitions.[30,31] The glass transition of CTA was followed by an exothermic transition at peak temperature 212 °C. Freshly prepared CTA sample, CTA sample vacuum heated at 60 °C, and CTA sample prepared from fibrous CTA also displayed this exothermic transition. Therefore, this exothermic transition could be due to partial decompositional changes in the CTA chain. It is seen from Table 2 that T_{g1} and T_{g2} were shifted from 68.1 and 196.6 °C in pure CTA to 122.5 and 208.7 °C in CTA+Aliquat-336, respectively. The glass transition enthalpy (ΔH) corresponding to T_{g2} was also increased significantly from 4.3 to 26.6 J g^{-1}. These results suggest that Aliquat-336 may have polar interactions with CTA leading to higher crystalline phases in the PIM. The value of ΔH decreased as a function of the amount of TEHP in the PIM containing fixed proportion of CTA+Aliquat-336; see Table 2. This could be attributed to reduction of polar interactions of Aliquat-336 with CTA chains by TEHP leading to a good plasticization of the PIM, which was also observed in surface roughness analyses. As can be seen from Table 2, the glass transition of PIMs is also dependent on the nature of the plasticizer. The PIMs containing NPOE and DOP had different T_g and higher ΔH values than TEHP plasticized PIMs having the same weight fraction of the plasticizer. The higher ΔH values in NPOE and DOP plasticized membrane indicated more crystalline phases in the matrices of these membranes. In all the cases, the CTA crystalline phases were modified as indicated by a shift in T_g but did not disappear even in the PIMs containing as high as 55 wt % of the plasticizer.

dx.doi.org/10.1021/jp1103615 |*J. Phys. Chem. B* 2011, 115, 5856–5867

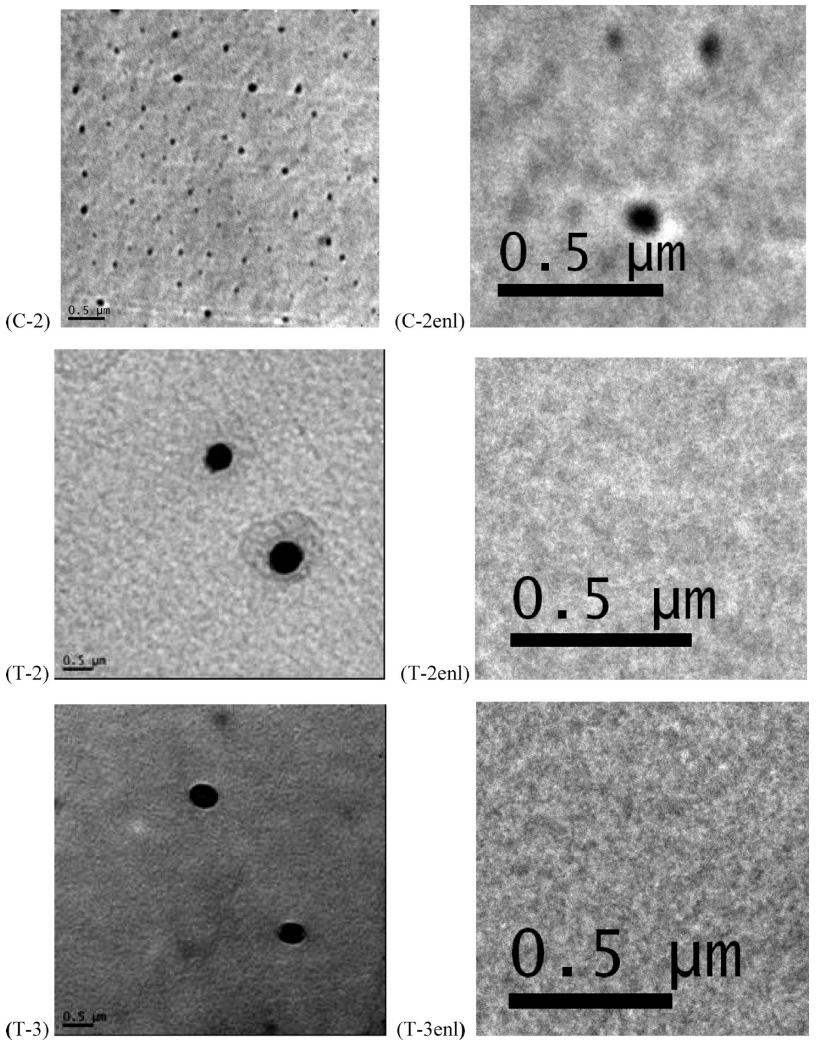

Figure 4. TEM images of cross section along the thickness of the Pt nanoparticles embedded membrane sample C-2 without plasticizer, sample T-2 with 44 wt % TEHP, and sample T-3 with 54 wt % TEHP. The enlarged images are marked as "enl". The black background is constituted by tiny Pt nanoparticles.

Thus, CTA could provide mechanical strength to the PIMs having high amount of the plasticizer.

To study the physical structure of the interior of the PIMs, the Pt nanoparticles (nps) were formed in membrane samples without plasticizer (C-2) and with varying amounts of TEHP plasticizer (T-2 and T-3). Since reductant BH_4^- is an anion, the Pt nps formed by in situ reduction of $PtCl_6^{2-}$ ions were expected to provide information on distribution of Aliquat-336 in the membrane. The TEM images of the cross section along the thickness of the membrane samples are shown in Figure 4. The TEM images of C-2, T-2, and T-3 membrane samples showed two types of Pt nps size distributions. The mostly smaller Pt nps were seen that formed uniform black background in the TEM images of all the membrane samples shown in Figure 4. X-ray diffraction patterns of the membrane samples containing Pt nps are shown in Figure 5. The broad peaks at scattering angles (2θ) correspond to the 111, 200, 220, 311, and 222 planes of face-centered cubic phase of Pt (JCPDS card no. 04-0802). The peak width of the (111) plane of Bragg reflection was analyzed to estimate the size of Pt nps embedded in the membrane using the Debye−Scherrer equation.[32] The size of Pt nps was estimated to be of the order of 4 nm for samples containing CTA+Aliquat-336 (C-2) and 7 nm for samples containing CTA+Aliquat-336+TEHP (T-2 and T-3). The uniform distribution of Pt nps in samples seems to suggest that carrier (Aliquat-336) molecules were uniformly distributed across the thickness of the membranes. The bigger Pt nps were few and appear to be formed by agglomeration of nps in voids or defects in the membrane sample. As can be seen from Figure 4, the density of bigger Pt nps (80−100 nm size) was higher in the unplasticized membrane as compared to the plasticized samples. The density of the bigger sized Pt nps was considerably reduced in the plasticized membranes (T-2 and T-3), but the size increased to 200−400 nm. The comparison of TEM images with AFM images given in Figure 2 indicated that the plasticization may have removed the voids and defects at the interior of the membrane due to swelling of CTA nodes. However, a small number of bigger defects still remained due to imperfect packing of swollen CTA blobs. In any case, the voids did not seem to be interconnected. Thus, the plasticized polymer inclusion membrane has homogeneous organic gel-like structure.

dx.doi.org/10.1021/jp1103615 |*J. Phys. Chem. B* 2011, 115, 5856–5867

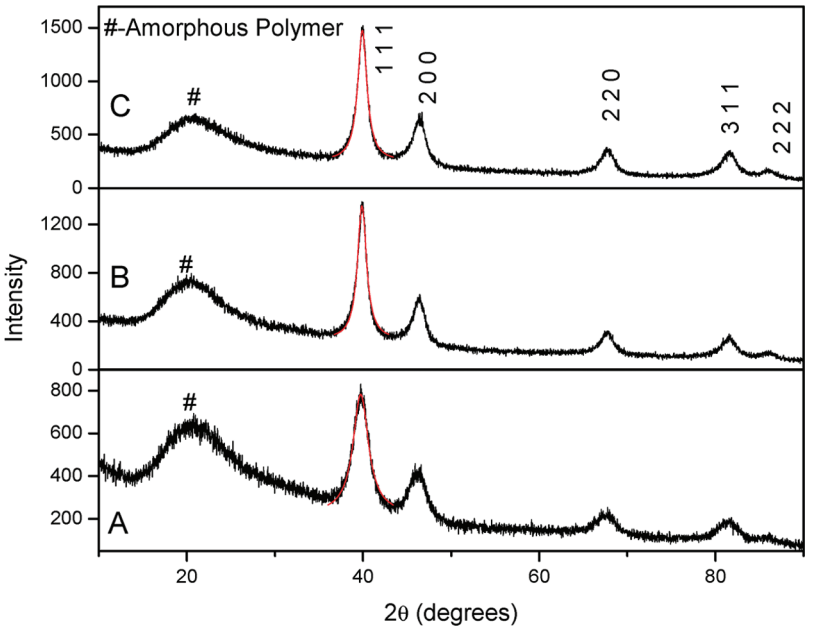

Figure 5. X-ray diffraction patterns of the PIMs having Pt nanoparticles embedded in matrices of (A) sample C-2 without plasticizer, (B) sample T-2 with 44 wt % TEHP, and (C) sample T-3 with 54 wt % TEHP.

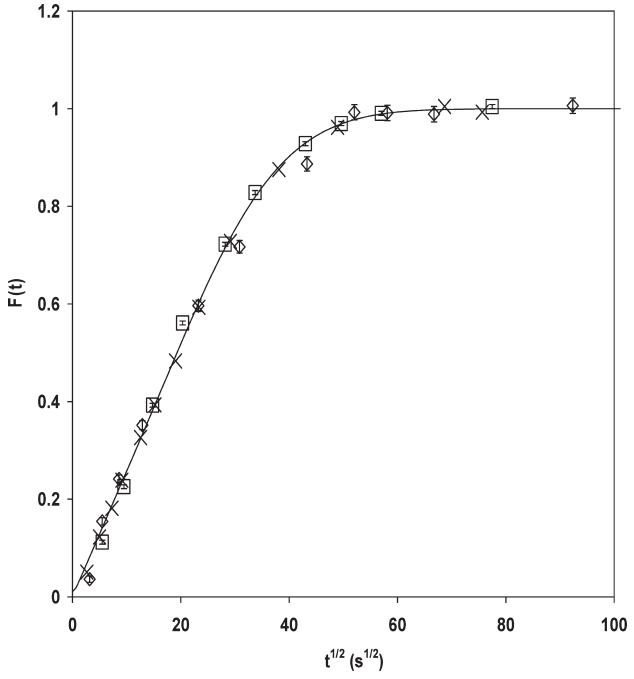

Figure 6. Fractional attainment of isotopic-exchange equilibrium $F(t)$ of I^- ions between membrane sample (PIM-1) and well-stirred 0.1 mol L^{-1} KI solution as a function of square root of equilibration time $t^{1/2}$. The symbols represent different sets of repeated experiment. The solid line represents the fitted data in terms of eq 3 for deducing the self-diffusion coefficient of I^- ions in the membrane.

Effects of Plasticizer on Diffusion Mobility. Plasticizer in the PIM also acts as a solvent for the carrier Aliquat-336. Therefore, the nature and amount of the plasticizer are expected to influence the intrinsic diffusion property of the PIM. In our previous studies, the variation of the self-diffusion coefficients of I^- ions ($D(I^-)$) in the PIM containing fixed proportions of CTA and Aliquat-336 and varying amounts of the plasticizer NPOE was studied.[18c] In this study, it was observed that log $D^m(I^-)$ increased linearly with increase in liquid volume fraction (NPOE+Aliquat-336) in the PIM sample. The polymer chains of CTA in the liquid fraction of PIM matrix offer obstruction in the path of the moving ions. This obstruction is reduced with increase in liquid fraction in the PIM. This fact is also corroborated by the microscopy studies discussed above. The plasticizer is a major component of the liquid phase and acts as a medium for diffusional transport of ions in the PIM. In the present work, the self-diffusion coefficients of I^- ions and water were measured in the PIM samples having fixed proportion of different plasticizers. The values of self-diffusion coefficients were obtained by least-squares fit of the profiles of fractional attainment of $^{131}I^-$ and HTO exchange equilibriums ($F(t)$) between membrane sample and well-stirred solution as a function of equilibration time (t) using eq 3 as described in the Experimental section. The representative experimental and fitted profiles of $F(t)$ as a function of equilibration time are shown in Figure 6, and the values of D for I^- ions and H_2O obtained from the analyses of the exchange profiles are given in Table 3. It is evident from Figure 6 that $F(t)$ varied as a function of square root of equilibration time $t^{1/2}$ up to attainment of 70% of exchange equilibrium, which is characteristic of the Fickian diffusion.

As seen from Table 3, the maximum value of $D(I^-)$ was 3.2×10^{-8} cm^2 s^{-1} in the membrane sample N-3 consisting of CTA, NPOE, and Aliquat-336. This value is 3 orders of magnitude lower than the self-diffusion coefficient of I^- ions (2.05×10^{-5} cm^2 s^{-1}) in aqueous medium.[33] The value of $D(I^-)$ was found to be 2.91×10^{-7} cm^2 s^{-1} in hydrophilic anion-exchange membrane that is also ≈10 times higher than the value of $D(I^-)$ in PIM.[34] This seems to suggest that anions diffusion in the PIM is a quite slow process. This may be due to the viscosity of the liquid fraction in the PIM as well as the homogeneous gel-like physical structure of the membrane. The comparison of the

dx.doi.org/10.1021/jp1103615 |J. Phys. Chem. B 2011, 115, 5856–5867

Table 3. Self-Diffusion Coefficients of I^- Ions and Water in the PIM Samples Having Different Plasticizers

	plasticizer[a]				
id.	type	dielectric constant	viscosity (cP)	$D(I^-)$ ($cm^2\ s^{-1}$)	$D(H_2O)$ ($cm^2\ s^{-1}$)
N-3	NPOE	24	13.1	$(3.2 \pm 0.7) \times 10^{-8}$ [b]	$(1.9 \pm 0.1) \times 10^{-7}$
T-3	TEHP	4.8	11.1	$(1.3 \pm 0.1) \times 10^{-8}$	$(1.3 \pm 0.2) \times 10^{-7}$
D-3	DOP	5.1	40.4	$(2.5 \pm 0.5) \times 10^{-9}$	$(1.2 \pm 0.2) \times 10^{-7}$

[a] Taken from refs 10a and 35. [b] From ref 18c.

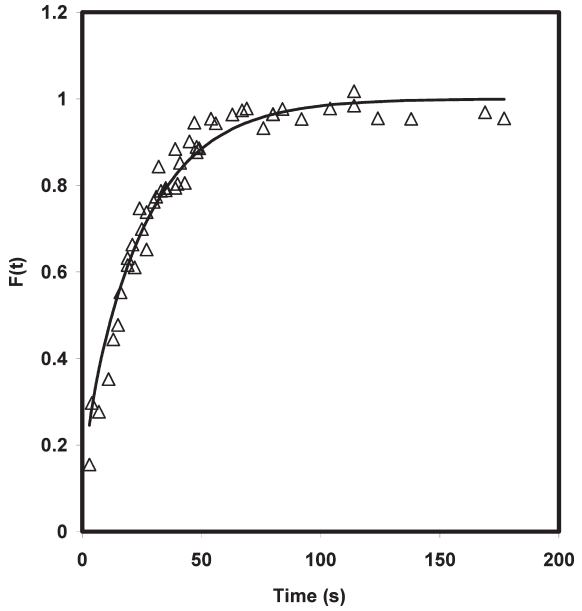

Figure 7. Fractional attainment of HTO-exchange equilibrium between equilibrating water and PIM sample in Cl^- form (N-3). Symbol and solid line represent experimental (normalized data of three experiments) and fitted data using eq 3, respectively.

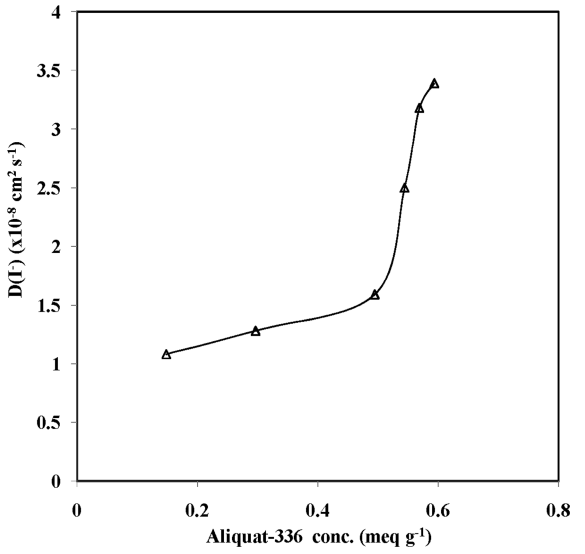

Figure 8. Variation of self-diffusion coefficients of I^- ions as a function of Aliquat-336 concentration in the membrane samples having fixed proportion (1:1) of CTA and NPOE. The concentration of Aliquat-336 in the membrane was varied by keeping of the amount of CTA = 0.40 ± 0.01 g, NPOE = 0.40 ± 0.01, and varying amount of Aliquat-336 from 0.05 to 0.26 g in 9 cm diameter membrane.

values of $D(I^-)$ of PIMs having the same fractions of the components but different plasticizers indicated that the intrinsic properties of the plasticizer strongly influence diffusion of I^- ions in the membrane matrix. For example, the PIMs consisting of NPOE (N-3), TEHP (T-3), and DOP (D-3) were found to have $D(I^-)$ in following order: 3.2×10^{-8} $cm^2\ s^{-1} > 1.3 \times 10^{-8}$ $cm^2\ s^{-1} \gg 2.5 \times 10^{-9}$ $cm^2\ s^{-1}$, respectively. The values of dielectric constant (ε_r) and viscosity of the plasticizers are given in Table 3.[10a,35] It is evident from Table 3 that the self-diffusion coefficient of I^- ions is highest in the sample made up of the plasticizer (NPOE) having higher ε_r and lower viscosity. Therefore, the values of $D(I^-)$ in following NPOE > TEHP > DOP order indicate that both viscosity and ε_r of the plasticizer affect diffusion mobility of ions in the PIM matrix. The viscosity is known to influence the diffusion mobility of ions in liquid medium as described by Stokes–Einstein and Eyring's equations.[33] The greater local dielectric constant would lead to lower activation barrier for the anions to hop between positively charged sites.

The measurement of the self-diffusion coefficient of water in the PIMs by radiotracer (HTO) was based on the assumption that the exchange occurs via displacement of HTO by H_2O in the membrane in contact with equilibrating water. This means that tritium transfer from a water molecule to another in pure water is negligible, and the isotopic effect on diffusion mobility is also within the uncertainty limit of the experimental measurements. The validity of these assumptions was based on the fact that the values of the self-diffusion coefficients of water traced by three isotopes D, T, and ^{18}O were found to be very close to each other.[36] Therefore, the HTO-exchange rate profiles were analyzed using eq 3 to deduce self-diffusion coefficients of water in the PIMs. The comparison of experimental data and fitted data is shown in Figure 7. The self-diffusion coefficients of water $D(H_2O)$ measured in the PIMs samples having different plasticizers are given in Table 3. The self-diffusion coefficients of water in the PIMs are considerably lower than the self-diffusion coefficient of water in pure water (2.5×10^{-5} $cm^2\ s^{-1}$ at 25 °C).[37] As values of $D(H_2O)$ are one magnitude higher than the values $D(I^-)$ ions in the membrane, the bulk water may be diffusing independent of the counterions. The apparent water diffusion coefficient in NPOE-plasticized PVC-based PIM was reported to be 2×10^{-8} $cm^2\ s^{-1}$.[38] This can be attributed to clustering of water in PVC-based PIM.[38,39] There is a trend in the variation of $D(H_2O)$ with counterions in the membrane, though values are not drastically different. The comparison of data given in Table 3 indicates that the value of $D(H_2O)$ in the N-3 sample is slightly higher than that in T-3 and D-3 membranes. This may

Table 4. Self-Diffusion Mobility of Anions in PIM (Sample N-3) with Respect to Iodide Ions ($D(X^-)/D(I^-)$) As Obtained by Electrochemical Impedance Spectroscopy (EIS)

counter ions (X^-)	resistance (KΩ)	$D(X^-)/D(I^-)$
I^-	1.02 ± 0.10	1.00
Cl^-	1.01 ± 0.10	1.11
NO_3^-	0.42 ± 0.05	1.66
SO_4^{2-}	0.86 ± 0.10	0.45

be due to higher dielectric constant of the NPOE than TEHP and DOP; see Table 3.

Effects of Concentration of Carrier on Diffusion Mobility. The other component of PIMs that can influence diffusion mobility of the ions is concentration of the carrier (Aliquat-336) in membrane. To study the effects of Aliquat-336 concentration on diffusion mobility, the values of $D(I^-)$ in the PIMs having constant proportion of CTA and NPOE (1:1) and varying concentration of Aliquat-336 were deduced from $(^*I^-)_m \rightleftarrows (I^-)_{aq}$ exchange rate profiles as discussed above, and data are plotted in Figure 8. As can be seen from this figure, the values of $D(I^-)$ did not vary significantly up to 0.5 mequiv g^{-1} concentration of Aliquat-336 in the PIM. Thereafter, it increased significantly from $(1.59 \pm 0.09) \times 10^{-8}$ cm^2 s^{-1} to $(3.18 \pm 0.08) \times 10^{-8}$ cm^2 s^{-1} at 0.6 mequiv g^{-1} concentration of Aliquat-336 in the membrane. Fontas et al. also observed similar variation of $PtCl_6^{2-}$ anions initial flux vs Aliquat-336 weight per unit area of the membrane consisting of NPOE plasticized CTA.[10b] They observed that a Aliquat-336 concentration threshold is required to give a significant flux of Pt(IV) anionic species across the PIM. After the threshold, initial flux varied linearly with Aliquat-336 concentration.[10b] It is expected that the value of $D^m(I^-)$ would not change with Aliquat-336 concentration if the transport of anions occurs only through the carrier diffusion process. In PIMs studied in the present work, the values of $D(I^-)$ varied with amount of the plasticizer as well as its viscosity. These are characteristics of the "carrier-diffusion" process. The variation of $D(I^-)$ as a function of Aliquat-336 obtained in the present work showed a Aliquat-336 concentration threshold barrier in I^- ions diffusion. This indicated involvement of "fixed-site hopping" in the transport process. The increase in value of $D(I^-)$ with dielectric constant of plasticizer also supports a fixed-site hopping mechanism. Therefore, the mechanism of transport is neither pure carrier-diffusion nor fixed-site hopping. It may be intermediate between these two processes, i.e., a "mobile-site hopping mechanism". The mobile-site hopping transport mechanism would involve limited diffusion mobility of the carrier Aliquat-336 as well as hopping of anions between the mobile carriers. This is expected as Aliquat-336 has three long hydrocarbon chains, and its diffusion mobility may be limited in the high-viscosity liquid channels.

Electrochemical Characterization. Bulk resistance of N-3 membrane sample, loaded with different anions, was measured using the EIS technique.[31] It is seen from the data given in Table 4 that bulk resistance of the membrane sample varied significantly with different counterions. The membrane sample with NO_3^- counterions was found to have lower resistance as compared to the samples with Cl^-, I^-, or SO_4^{2-} counterions. This seems to indicate that NO_3^- ions have higher mobility in PIM than other anions. To understand variation in the self-diffusion mobility of anions in PIM, the data obtained from the

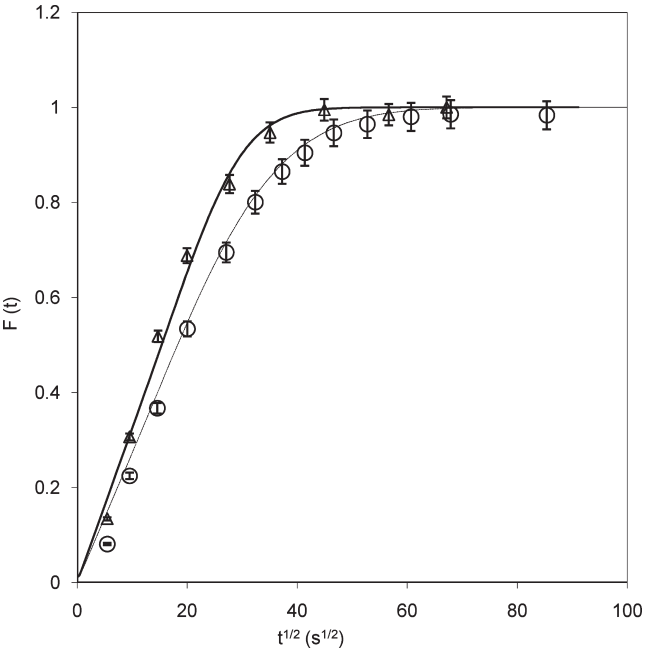

Figure 9. Profiles of fractional attainment of NO_3^- exchange equilibrium $F(t)$ with I^- ions in membrane sample (N-3) as a function of square root of equilibration time t. The symbols Δ and O represent $(NO_3^-)_{mem} \rightleftarrows (I^-)_{aq}$ and $(I^-)_{mem} \rightleftarrows (NO_3^-)_{aq}$ exchanges, respectively. The solid and broken lines represent the predicted $(NO_3^-)_{mem} \rightleftarrows (I^-)_{aq}$ and $(I^-)_{mem} \rightleftarrows (NO_3^-)_{aq}$ exchange profiles, respectively, using the Nernst–Planck equation for interdiffusion of the exchanging counterions.

EIS was used to calculate the self-diffusion coefficients of anions, and normalized with the self-diffusion coefficient of I^- ions in the same membrane. The normalization with respect to I^- ions was done as the self-diffusion coefficient of I^- ions in N-3 membrane sample was accurately measured by the radiotracer method. Among the four anions studied, NO_3^- ions were found to have the highest mobility and SO_4^{2-} ions had the lowest mobility in the membrane. The mobilities of Cl^- and I^- ions were almost comparable. SO_4^{2-} ions are expected to bind with two anion-exchanger molecules. Therefore, it showed lower mobility as compared to that of the monovalent anions.

Counterion-Exchange Kinetics. The fluxes of the interchanging counterions are governed by their interdiffusion coefficients in the membrane matrix, which changes as the ion-exchange progresses. The Nernst–Planck theory of ionic motions predicts different rates of forward $(A^{n+})_{mem} \rightleftarrows (B^{n+})_{aq}$ and reverse exchange $(B^{n+})_{mem} \rightleftarrows (A^{n+})_{aq}$ in the case where interchanging ions do not have same diffusion coefficients.[40] If the ion "A" initially present in the membrane has higher diffusion coefficient than the ion "B" (initially in the solution), then the exchange of A for B is faster than the reverse process, when B is exchanged for A. In present work, NO_3^- and Cl^- anions forward and reverse exchanges with I^- ions were studied. The experimentally measured counterion-exchange rate profiles are shown in Figures 9 and 10. As seen in these figures, the forward $(I^-)_{mem} \rightleftarrows (NO_3^-)_{aq}$ and reverse $(NO_3^-)_{mem} \rightleftarrows (I^-)_{aq}$ exchange rate profiles are different, but forward and reverse exchange rate profiles of Cl^- with I^- ions are almost similar. This is because NO_3^- ions have 1.66 times faster diffusion mobility than I^- ions in the same membrane; see Table 4. Cl^- and I^- ions have

dx.doi.org/10.1021/jp1103615 |J. Phys. Chem. B 2011, 115, 5856–5867

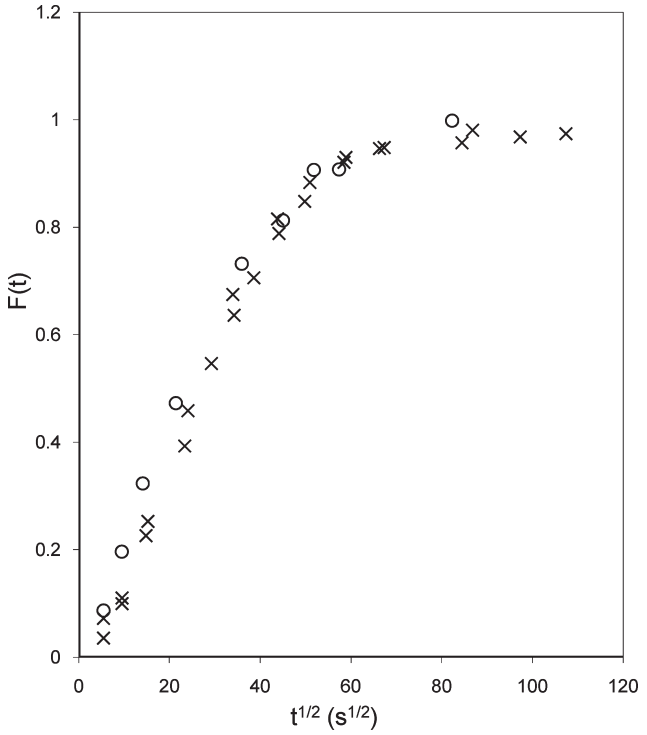

Figure 10. Profiles of fractional attainment of Cl^- exchange equilibrium $F(t)$ with I^- ions in membrane sample (N-3) as a function of square root of equilibration time t. The symbols × and ○ represent $(Cl^-)_{mem} \rightleftarrows (I^-)_{aq}$ and $(I^-)_{mem} \rightleftarrows (Cl^-)_{aq}$ exchanges, respectively.

comparable diffusion mobility, which would result in similar forward and reverse exchange rate profiles. The forward and reverse exchange rate profiles of ClO_4^- ions with I^- were also found to be identical indicating similar diffusion mobility of ClO_4^- and I^- ions; see the Supporting Information.

A numerical solution of the Nernst−Planck (N−P) equation for interdiffusion was used to study the kinetics of NO_3^- ions exchanges with I^- ions. The details of procedure are given elsewhere.[40] In this analyses, the exchange rate profiles were obtained using values $D(I^-)$ and ratio $D(NO_3^-)/D(I^-)$ given in the Tables 3 and 4, respectively. A reasonably good agreement between experimental and predicted exchange rate profiles clearly indicates that NO_3^- ions indeed have higher mobility in PIMs than the Cl^- and I^- ions.

CONCLUSIONS

The microscopy studies showed that PIMs are homogeneous gel-like membranes due to swelling of CTA chains with plasticizer. The plasticizer was found to influence physical structure as well as diffusion mobility of the ions in the membrane matrix. The study on glass transitions of the PIMs indicated that crystalline phases of CTA were modified on inclusion of Aliquat-336 and different plasticizer but did not disappear even on inclusion of high amount of the plasticizer. Thus, CTA could provide mechanical strength to highly plasticized membrane. The ion-exchange capacities of the PIMs studied in the present work were found to be dependent on concentration of the liquid anion-exchanger (Aliquat-336) and did not change significantly with the nature and amount of the plasticizer. The self-diffusion mobility of I^- ions in the PIM was found to be affected by dielectric constant and viscosity of the plasticizer used in preparation of the PIM. The variation of $D(I^-)$ as a function of Aliquat-336 concentration seems to suggest that diffusion mechanism of anions in the PIMs is by "mobile-site hopping". Therefore, the amount of the carrier and nature of the plasticizer play an important role in the transport process in PIMs. The self-diffusion coefficients of water in PIMs were found to be one magnitude higher than the self-diffusion coefficients of iodide ions. This indicated that water molecules diffuse independently across the PIM. The electrochemical impedance spectroscopic and counterion-exchange kinetics studies indicated the variation of self-diffusion mobility of anions in the following order: $NO_3^- > Cl^- \approx I^- \approx ClO_4^- > SO_4^{2-}$.

ASSOCIATED CONTENT

Supporting Information. Experimental setup; $ClO_4^- \leftrightarrow I^-$ exchange rate profile; impedance spectra. This material is available free of charge via the Internet at http://pubs.acs.org.

AUTHOR INFORMATION

Corresponding Author

*Fax +91-22-25505150/25505151; tel. +91-22-25590641; e-mail ashokk@barc.gov.in.

ACKNOWLEDGMENT

The authors thank Mr. Rakesh Shukla, Chemistry Division, BARC for carrying out XRD analyses. The authors also thank the CryoTEM Facility of IIT Bombay for TEM access.

REFERENCES

(1) (a) Kubota, F.; Goto, M. *Sol. Extract. Res. Dev.* **2005**, *12*, 11–16. (b) Walkowiak, W.; Kozlowski, C. A. *Desalination* **2009**, *240*, 186–197. (c) Yang, X. J.; Fane, A. G.; Soldenhoff, K. *Ind. Eng. Chem. Res.* **2003**, *42*, 392–403.

(2) Barboiu, M.; Cazacu, A.; Michau, M.; Caraballo, R.; Arnal-Herault, C.; Pasc-Banu, A. *Chem. Eng. Process.* **2008**, *47*, 1044–1052.

(3) Lamb, J. D.; Morris, C. A.; West, J. N.; Morris, K. T.; Harrison, R. G. *J. Membr. Sci.* **2008**, *321*, 15–21.

(4) (a) Kocherginsky, N. M.; Yang, Q; Seelam, L. *Sep. Purif. Technol.* **2007**, *21*, 171–177. (b) Vilt, M. E.; Ho, W. S. W. *J. Membr. Sci.* **2009**, *342*, 80–87. (c) Hernandez-Fernandez, F. J.; Rios, A. P. d.; Tomas-Alonso, F.; Palacios, J. M.; Villora, G. *J. Membr. Sci.* **2009**, *341*, 172–177. (d) de Gyves, J.; Miguel, E. R. d. S. *Ind. Eng. Chem. Res.* **1999**, *38*, 2182–2202. (e) Canet, L.; Vanel, P.; Aouad, N.; Tronel-Peyroz, E.; Palmeri, J.; Seta, P. *J. Membr. Sci.* **1999**, *163*, 109–121.

(5) (a) Lee, J.; Lee, H. K.; Rasmussen, K. E.; Pedersen-Bjergaar, S. *Anal. Chim. Acta* **2008**, *624*, 253–268. (b) Arce, L.; Nozal, L.; Simonet, B. M.; Rios, A.; Valcarcel, M. *Trends Anal. Chem.* **2009**, *28*, 842–853. (c) Zhang, Z.; Buffle, J.; van Leeuwen, H. P.; Wojciechowski, K. *Anal. Chem.* **2006**, *78*, 5693–5703.

(6) (a) Kemperman, A. J. B.; Bargeman, D.; Boomgaard, Th. V. D.; Strathmann, H. *Sep. Sci. Technol.* **1996**, *31*, 2733–2762. (b) Yang, X. J.; Fane, A. G.; Bi, J.; Griesser, H. J. *J. Membr. Sci.* **2000**, *168*, 29–37. (c) Zheng, H.-D.; Wang, B.-Y.; Wu, Y.-X.; Ren, Q.-L. *Colloids Surf., A* **2009**, *351*, 38–45. (d) Fortunato, R.; Afonso, C. A. M.; Benavente, J.; Rodriguez-Castellon, E.; Crespo, J. G. *J. Membr. Sci.* **2005**, *256*, 216–223. (e) Dastgir, M. G.; Peeva, L. G.; Livingston, A. G.; Morley, T. A.; Steinke, J. H. G. *Ind. Eng. Chem. Res.* **2005**, *44*, 7659–7667.

(7) Ulbricht, M. *Polymer* **2006**, *47*, 2217−2268 and references therein.

(8) (a) Thunhorst, K. L.; Noble, R. D.; Bowman, C. N. *J. Membr. Sci.* **1999**, *156*, 293–302. (b) Elliott, B. J.; Willis, W. B.; Bowman, C. N.

J. Membr. Sci. **2000**, *168*, 109–119. (c) Duhart, A.; Dozol, J. F.; Rouquette, H.; Deratani, A. *J. Membr. Sci.* **2001**, *185*, 145–155. (d) Vasudevan, T.; Das, S.; Debnath, A. K.; Pandey, A. K. *J. Membr. Sci.* **2009**, *342*, 113–120.

(9) (a) Nghiem, L. D.; Mornane, P.; Potter, I. D.; Perera, J. M.; Cattrall, R. W.; Kolev, S. D. *J. Membr. Sci.* **2006**, *281*, 7–41. (b) Walkowiak, W.; Bartsch, R. A.; Kozloski, C.; Gega, J.; Charewicz, W. A.; Amiri-Eliasi, B. *J. Radioanal. Nucl. Chem.* **2000**, *246*, 643–650. (c) Sugiura, M. *Sep. Sci. Technol.* **1993**, *28*, 1453–1463. (d) de San Miguel, E. R.; Hernandez-Andaluz, A. Ma.; Banuelos, J. G.; Saniger, J. M.; Aguilar, J. C.; de Gyves, J. *Mater. Sci. Eng., A* **2006**, *434*, 30–38. (e) Kim, J. S.; Kim, S. K.; Ko, J. W.; Kim, E. T.; Yu, S. H.; Cho, M. H.; Kwon, S. G.; Lee, E. H. *Talanta* **2000**, *52*, 1143–1148.

(10) (a) Scindia, Y. M.; Pandey, A. K.; Reddy, A. V. R. *J. Membr. Sci.* **2005**, *249*, 143–152. (b) Fontas, C.; Tayeb, R.; Tingry, S.; Hidalgo, M.; Seta, P. *J. Membr. Sci.* **2005**, *263*, 96–102. (c) Aguilar, J. C.; Sanchez-Castellanos, M.; Miguel, E. R. d. S.; Gyves, J. de *J. Membr. Sci.* **2001**, *190*, 107–118.

(11) (a) Bakker, E.; Bühlmann, P.; Pretsch, E. *Chem. Rev.* **1997**, *97*, 3083–3132. (b) Pretsch, E.; Bühlmann, P.; Bakker, E. *Chem. Rev.* **1998**, *98*, 1593–1687. (c) Adhikari, B.; Mjumdar, S. *Prog. Polym. Sci.* **2004**, *29*, 699–766. (d) Eugster, R.; Rosatzin, T.; Rusterholz, B.; Aebersold, B.; Pedrazza, U.; Ruegg, D.; Schmid, A.; Spichiger, U. E.; Simon, W. *Anal. Chim. Acta* **1994**, *289*, 1–13.

(12) Sakai, Y.; Kadota, K.; Hayashita, T.; Cattrall, R. W.; Kolev, S. D. *J. Membr. Sci.* **2010**, *346*, 250–255.

(13) Gardner, J. S.; Walker, J. O.; Lamb, J. D. *J. Membr. Sci.* **2004**, *229*, 87–93.

(14) Ye, Q.; Borbely, S.; Horvai, G. *Anal. Chem.* **1999**, *71*, 4313–4320.

(15) Tripathi, R.; Pandey, A. K.; Sodaye, S.; Tomar, B. S.; Manohar, S. B.; Santra, S.; Mahata, K.; Singh, P.; Kailas, S. *Nucl. Instrum. Methods Phys. Res., Sect. B* **2003**, *211*, 138–144.

(16) Fontas, C.; Tayeb, R.; Dhahbi, M.; Gaudichet, E.; Thominette, F.; Roy, P.; Steenkeste, K.; Fontaine-Aupart, M.-P.; Tingry, S.; Tronel-Peyroz, E.; Seta, P. *J. Membr. Sci.* **2007**, *290*, 62–72.

(17) Miguel, E. R.; de, S.; Aguilar, J. C.; Gyves, J. d. *J. Membr. Sci.* **2008**, *307*, 105–116.

(18) (a) Fiedler, U. *Anal. Chim. Acta* **1977**, *89*, 111–118. (b) Sodaye, S.; Suresh, G.; Pandey, A. K.; Goswami, A. *J. Membr. Sci.* **2007**, *295*, 108–113. (c) Sodaye, S.; Suresh, G.; Pandey, A. K.; Goswami, A. *Radiochim. Acta* **2006**, *94*, 347–350. (d) Levitskaia, T. G.; Macdonald, D. M.; Lamb, J. D.; Moyer, B. A. *Phys. Chem. Chem. Phys.* **2000**, *2*, 1481–1491.

(19) Riggs, J. A.; Smith, B. D. *J. Am. Chem. Soc.* **1997**, *119*, 2765–2766.

(20) Munro, T. A.; Smith, B. D. *J. Chem. Soc., Chem. Commun.* **1997**, *22*, 2167–2168.

(21) Paugam, M. F.; Buffle, J. *J. Membr. Sci.* **1998**, *147*, 207–215.

(22) White, K. M.; Smith, B. D.; Duggan, P. J.; Sheahan, S. L.; Tyndall, E. M. *J. Membr. Sci.* **2001**, *194*, 165–175.

(23) Malewitz, T.; Pintauro, P. N.; Rear, D. *J. Membr. Sci.* **2007**, *301*, 171–179.

(24) Gardner, J. S.; Peterson, Q. P.; Walker, J. O.; Jensen, B. D.; Adhikary, B.; Harrison, R. G.; Lamb, J. D. *J. Membr. Sci.* **2006**, *277*, 165–176.

(25) Goswami, A.; Acharya, A.; Pandey, A. K. *J. Phys. Chem. B* **2001**, *105*, 9196–9201.

(26) Kumar, R.; Pandey, A. K.; Tyagi, A. K.; Dey, G. K.; Ramagiri, S. V.; Bellare, J. R.; Goswami, A. *J. Colloid Interface Sci.* **2009**, *337*, 523–530.

(27) Armstrong, R. D.; Covington, A. K.; Proud, W. G. *J. Electroanal. Chem.* **1988**, *257*, 155–160.

(28) Millet, P. *J. Membr. Sci.* **1990**, *50*, 325–328.

(29) Suresh, G.; Scindia, Y. M.; Pandey, A. K.; Goswami, A. *J. Membr. Sci.* **2005**, *250*, 39–45.

(30) Daane, J. H.; Barker, R. E., Jr. *Polym. Lett.* **1964**, *2*, 343–347.

(31) Arous, O.; Amara, M.; Kerdjoudj, H. *J. Appl. Polym. Sci.* **2004**, *93*, 1401–1410.

(32) Klug, H. P.; Alexander, L. E. *X-ray Diffraction Procedures*; John Wiley and Sons: New York, 1959.

(33) Robinson, R. A.; Stokes, R. H. *Electrolyte Solutions*, second ed.; Butterworths: London, 1965.

(34) Pandey, A. K.; Goswami, A.; Sen, D.; Mazumder, S.; Childs, R. F. *J. Membr. Sci.* **2003**, *217*, 117–130.

(35) Keplinger, F. J.; Jachimowicz, A.; Kohl, F. *Anal. Chem.* **1998**, *70*, 4271–4279.

(36) Thau-Alexandrowicz, G. *J. Membr. Sci.* **1978**, *4*, 151–163.

(37) Easteal, A. J.; Vernon, A.; Edge, J.; Wolf, L. A. *J. Phys. Chem.* **1984**, *88*, 6060–6063.

(38) Zwicki, T.; Schneider, B.; Lindner, E.; Sokalski, T.; Schaller, U.; Pretsch, E. *Anal. Sci.* **1998**, *14*, 57–61.

(39) Chan, A. D. C.; Li, X.; Harrison, D. J. *Anal. Chem.* **1992**, *64*, 2512–2517.

(40) (a) Suresh, G.; Scindia, Y. M.; Pandey, A. K.; Goswami, A. *J. Phys. Chem. B* **2004**, *108*, 4104–4110. (b) Sodaye, S.; Suresh, G.; Pandey, A. K.; Goswami, A. *J. Phys. Chem B* **2009**, *113*, 12482–12488.